1
Introduction

A plasma is a many body system consisting of a huge number of interacting (charged and neutral) particles. More precisely, one defines a plasma as a quasineutral gas of charged and neutral particles which exhibits collective behavior. In many cases, one considers quasineutral gases consisting of charged particles, namely electrons and positively charged ions of one species. Plasmas may contain neutral atoms. In this case, the plasma is called partially or incompletely ionized. Otherwise the plasma is said to be completely or fully ionized. The term plasma is not limited to the most common electron–ion case. One may have electron–positron plasmas, quark-gluon plasmas, and so on. Semiconductors contain plasma consisting of electrons and holes.

Most of the matter in the universe occurs in the plasma state. It is often said that 99% of the matter in the universe is in the plasma state. However, this estimate may not be very accurate. Remember the discussion on dark matter. Nevertheless, the plasma state is certainly dominating the universe.

Modern plasma physics emerged in 1950s, when the idea of thermonuclear reactor was introduced. Fortunately, modern plasma physics completely dissociated from weapons development. The progression of modern plasma physics can be retraced from many monographs, for example, [1–15].

In simple terms, plasmas can be characterized by two parameters, namely, charged particle density n and temperature T. The density varies over roughly 28 orders of magnitude, for example, from 10^6 to 10^{34} m^{-3}. The kinetic energy $k_B T$, where k_B is the Boltzmann constant, can vary over approximately seven orders, for example, from 0.1 to 10^6 eV.

The notation "plasma" was introduced by Langmuir, Tonks, and their collaborators in the 1920s when they studied processes in electronic lamps filled with ionized gases, that is, low-pressure discharges. The word "plasma" seems to be a misnomer [16]. The Greek $\pi\lambda\acute{\alpha}\sigma\mu\alpha$ means something modeled or fabricated. However, a plasma does not tend to generally conform to external influences. On the contrary, because of collective behavior, it often behaves as if it had a mind of its own [16].

Plasmas appear in space and astrophysics [17–19], laser–matter interaction [20, 21], technology [22], fusion [14, 23–26], and so on. Technical plasmas, magnetic fusion plasmas, and laser-generated plasmas represent the main applications of

High Temperature Plasmas, Theory and Mathematical Tools for Laser and Fusion Plasmas, First Edition.
Karl-Heinz Spatschek.

plasma physics on earth. Space plasmas, as they appear, for example, in the magnetosphere of the earth are very important for our life on earth. A continuous stream of charged particles, mainly electrons and protons, called the solar wind impinges on the earth's magnetosphere which shields us from this radiation. Typical solar wind parameters are $n = 5 \times 10^6\,\mathrm{m}^{-3}$, $k_B T_i = 10\,\mathrm{eV}$, and $k_B T_e = 50\,\mathrm{eV}$. However, also temperatures of the order $k_B T = 1\,\mathrm{keV}$ may appear. The drift velocity is approximately 300 km/s.

We could present numerous other examples of important plasmas, for example, stellar interiors and atmospheres which are hot enough to be in the plasma state, stars in galaxies, which are not charged but behave like particles in a plasma, free electrons and holes in semiconductors which also constitute a plasma. However, before discussing some of these objects in more detail, let us concentrate first on basic theoretical tools for their description.

1.1 Quasineutrality and Debye Shielding

Negative charge fluctuations $\delta\rho = -e\delta n$ (e is the elementary charge) generate electrostatic potential fluctuations $\delta\phi$ (we use SI units; see Appendix A)

$$\nabla^2 \delta\phi = \frac{1}{\varepsilon_0} e\delta n \,. \tag{1.1}$$

A rough estimate gives

$$\nabla^2 \delta\phi \sim \frac{\delta\phi}{l^2} \,, \tag{1.2}$$

where l is the characteristic fluctuation scale. Thus,

$$\delta\phi \approx \frac{1}{\varepsilon_0} e\delta n l^2 \,. \tag{1.3}$$

On the other hand, the characteristic potential energy $-e\delta\phi$ cannot be larger than the mean kinetic energy of particles which we roughly approximate by $k_B T$ (we measure the temperature in kelvin, k_B is the Boltzmann constant, and we ignore numerical factors). Thus,

$$\frac{\delta n}{n} \lesssim \frac{\varepsilon_0 k_B T}{n e^2 l^2} \,. \tag{1.4}$$

We recognize that a typical length appears, namely, the Debye length (more details will be given within the next chapters)

$$\lambda_D = \sqrt{\frac{\varepsilon_0 k_B T}{n_e e^2}} \,, \tag{1.5}$$

such that

$$\frac{\delta n}{n} \lesssim \frac{\lambda_D^2}{l^2} \ . \tag{1.6}$$

A plasma is quasineutral on distances much larger than the Debye radius. If the plasma size is comparable with λ_D, then it is not a "real" plasma, but rather just a heap of charged particles.

The Debye length is the shielding length in a plasma (at the moment, we will not discuss which species, electrons or ions are dominating in the shielding process). Let us again start from the Poisson equation

$$\nabla^2 \phi = \frac{1}{\varepsilon_0} e\,(n_e - n_i) \ . \tag{1.7}$$

Assuming Boltzmann distributed electrons and ions (let us assume with the same temperature T which we measure in eV, that is, $k_B T \to T$), we have

$$n_e = n_{e0} e^{e\phi/T} \approx n_{e0}\left(1 + e\frac{\phi}{T}\right) \ , \quad n_i = n_{e0} e^{-e\phi/T} \approx n_{e0}\left(1 - e\frac{\phi}{T}\right) \ . \tag{1.8}$$

Anticipating spherical symmetry, we obtain

$$\nabla^2 \phi = \frac{d^2\phi}{dr^2} + \frac{2}{r}\frac{d\phi}{dr} = \frac{2e^2 n_{e0}}{\varepsilon_0 T}\phi \ . \tag{1.9}$$

This is a homogeneous linear differential equation. The amplitude parameter is free. It is easy to check that for $r \neq 0$, a solution is

$$\Phi = \frac{e}{r} e^{-\sqrt{2}r/\lambda_D} \ . \tag{1.10}$$

Thus, the potential in a plasma is exponentially shielded with the Debye length as the shielding distance.

However, the calculation is not yet complete. Thus far, the central charge q, which creates the shielding cloud, is missing. This is reflected in the fact that the amplitude is still free. It is obvious that instead of Eqs. (1.7) and (1.9), we should solve the following inhomogeneous linearized Poisson–Boltzmann equation, that is,

$$\begin{aligned} \nabla^2 \phi &= -\frac{1}{\varepsilon_0} q\delta(\boldsymbol{r}) - \frac{1}{\varepsilon_0}\sum_{s=e,i} q_s n_s \\ &\approx \kappa^2 \phi - \frac{1}{\varepsilon_0} q\delta(\boldsymbol{r}) \ , \end{aligned} \tag{1.11}$$

where the index s denotes the species, electrons and ions, the test charge q is sitting at $\boldsymbol{r} = 0$, and

$$\kappa^2 = \sum_s \frac{n_s q_s^2}{\varepsilon_0 T} \doteq \frac{2}{\lambda_D^2} \ . \tag{1.12}$$

Its solution is the screened Debye potential of the test charge q, that is,

$$\phi = \frac{1}{4\pi\varepsilon_0}\frac{q}{r}e^{-\kappa r}\,, \tag{1.13}$$

as expected. The easiest direct way for finding the solution is by Fourier transformation (see Appendix B)

$$\phi_k = \int d^3r e^{-i\boldsymbol{k}\cdot\boldsymbol{r}}\phi(\boldsymbol{r}) \tag{1.14}$$

which immediately leads to

$$\phi_k = \frac{1}{\varepsilon_0}\frac{q}{k^2+\kappa^2}\,. \tag{1.15}$$

Back-transformation gives

$$\begin{aligned}\phi(\boldsymbol{r}) &= \frac{1}{(2\pi)^3}\int d^3k e^{i\boldsymbol{k}\cdot\boldsymbol{r}}\phi_k = \frac{1}{4\pi\varepsilon_0}\frac{1}{\pi}\int_{-1}^{1}dx\int_0^\infty dk\,k^2\frac{q}{k^2+\kappa^2}e^{ikrx}\\ &= \frac{1}{4\pi\varepsilon_0}\frac{2}{\pi}\int_0^\infty dk\,k\frac{q}{k^2+\kappa^2}\frac{\sin(kr)}{r} = \frac{1}{4\pi\varepsilon_0}\frac{q}{r}e^{-\kappa r}\,,\end{aligned} \tag{1.16}$$

since

$$\int_0^\infty \frac{x^{2m+1}\sin(ax)}{(x^2+z)^{n+1}}dx = \frac{(-1)^{n+m}}{n!}\frac{\pi}{2}\frac{d^n}{dz^n}\left(z^m e^{-a\sqrt{z}}\right), \tag{1.17}$$

which we applied for $n = m = 0$, $a = r$, $x = k$, and $z = \kappa^2$.

In conclusion, let us calculate the induced space charge. We decompose the potential

$$\phi(r) = \frac{1}{4\pi\varepsilon_0}\frac{q}{r}e^{-\kappa r} = \phi^{Cb} + \phi^{ind}\,, \tag{1.18}$$

where

$$\phi^{ind} = \frac{1}{4\pi\varepsilon_0}\frac{q}{r}\left(e^{-\kappa r}-1\right). \tag{1.19}$$

The induced space charge ρ^{ind}, which is responsible for the shielding (compared to the "naked" Coulomb potential ϕ^{Cb}) follows from

$$\nabla^2\phi^{ind} \equiv \frac{1}{r^2}\frac{d}{dr}\left(r^2\frac{d\phi^{ind}}{dr}\right) = -\frac{1}{\varepsilon_0}\rho^{ind}\,. \tag{1.20}$$

A straightforward calculation leads to

$$\rho^{ind} = -\frac{q\kappa^2}{4\pi r}e^{-\kappa r}\,. \tag{1.21}$$

Integrating the induced space charge density, which expresses the polarization, we obtain the expected result

$$\int d^3 r \rho^{ind} = -q \, . \tag{1.22}$$

The sign of the shielding charge distribution is opposite to the sign of the test charge q. Shielding causes a redistribution of charges compared to the ideal plasma situation (in the latter, the interaction potential is neglected).

The picture of the Debye shielding is valid only if there are enough particles in the charge cloud. We can compute the number N_D of particles in a Debye sphere,

$$N_D = n \frac{4}{3} \pi \lambda_D^3 \, ; \tag{1.23}$$

effective shielding over a Debye length requires

$$N_D \gg 1 \, . \tag{1.24}$$

A plasma with characteristic dimension L can be considered quasineutral, provided

$$\lambda_D \ll L \, . \tag{1.25}$$

It is easy to show that the largest spherical volume of a plasma that spontaneously could become depleted of electrons has the radius of a few Debye lengths. Let us consider a sphere of uniformly distributed ions with density $n_i(\boldsymbol{r}) = \text{const}$. Starting from the center of the sphere, the radial coordinate r is being introduced. The charge $Q = 4\pi n_i e r^3/3$ is enclosed up to r, and the electric field only has a radial component

$$E_r = \frac{1}{4\pi\varepsilon_0} \frac{Q}{r^2} = \frac{n_i e r}{3\varepsilon_0} \, . \tag{1.26}$$

From here, we find the electrostatic field energy W in the sphere of radius r as

$$W = \frac{\varepsilon_0}{2} \int_0^r E_r^2 4\pi r^2 dr = \frac{2\pi r^5 n_i^2 e^2}{45\varepsilon_0} \, . \tag{1.27}$$

Let us now discuss the scenario that the ion-filled sphere has been created by evacuating electrons. Before leaving the sphere, the electrons had the kinetic energy

$$E_{kin} = \frac{3}{2} n_e T_e \times \frac{4}{3} \pi r^3 \, . \tag{1.28}$$

The electrostatic energy W did not exist when (neutralizing) electrons were initially in the sphere to balance the ion charge. In other words, W must be equivalent to the work done by electrons on leaving the sphere. E_{kin} was available to the electrons. By equating

$$W = E_{kin}, \tag{1.29}$$

we find the maximum radius or the largest spherical volume that could spontaneously become depleted of electrons. A short calculation leads to

$$r_{max}^2 = 45\varepsilon_0 \frac{T_e}{n_e e^2} \tag{1.30}$$

or

$$r_{max} \approx 7\lambda_{De} \,. \tag{1.31}$$

1.2 Degree of Ionization

A plasma may be partially or full ionized, respectively. The degree of ionization depends on several parameters. Let us first estimate the degree of ionization on the basis of thermal ionization in a system consisting of hydrogen (H) atoms, electrons (e), and protons (p) (ions).

1.2.1 The Saha Equation

The Saha equation gives a relationship between the free particles (for example, electrons and protons) and those bound in atoms (H). To derive the Saha equation, we assume thermodynamic equilibrium and *collisional ionization*. We choose a consistent set of energy levels. Let us choose $E = 0$ when the electron is free (unbound) and has velocity zero, and $E = E_n < 0$ when the electron is in a bound state of the hydrogen atom ($Z = 1$). Using the simple Bohr energy formula for $n = 1$, we ignore the higher n levels,

$$E_n = \frac{Z}{n^2} \times (-13.6\,\text{eV}) \,. \tag{1.32}$$

The first excited state is already close to the bound-free-limit when compared to the ground state. When sufficient energy is available to excite an electron from the ground state $n = 1$ to $n = 2$, only a little bit more (one third) is needed to directly ionize.

For independent particles, we first calculate the *single particle* partition functions for electrons, protons, and hydrogen atoms which have the form[1)] [27]

$$Z = \sum_n e^{-E(n)/k_B T} \,. \tag{1.33}$$

Here, the sum is over all states (bound and free) with energies $E(n)$. The sums in the partition functions are actually integrals for the free particles since the particles have a continuous momentum distribution. The degeneracy of states (or statistical

1) We keep the Boltzmann constant k_B as it is done in most books on statistical physics.

weights) g_i with $g_e = g_p = 2$ and $g_H = 4$ (for hydrogen) has to be taken into account. Therefore, for free electrons and free protons (ions), we have

$$Z_j = \frac{1}{h^3} \int g_j \, e^{[-p^2/(2m_j)]/(k_B T_j)} \, d^3r \, d^3p \quad \text{for} \quad j = e, p \; . \tag{1.34}$$

Because of isotropy, $d^3p = 4\pi p^2 \, dp$, the integrals can be performed, that is,

$$Z_e = \frac{2V}{h^3} \left(2\pi \, m_e k_B \, T_e\right)^{3/2} \; , \tag{1.35}$$

$$Z_p = \frac{2V}{h^3} \left(2\pi \, m_p k_B \, T_p\right)^{3/2} \; . \tag{1.36}$$

Here, m_e and m_p are the electron and proton masses, respectively. For the temperature, we have in equilibrium $T = T_e = T_p = T_H$. A similar calculation leads for freely moving hydrogen atoms consisting of a bound electron–proton pair (in the ground state) to

$$Z_H = \frac{4V}{h^3} \left(2\pi \, m_H k_B \, T_H\right)^{3/2} e^{E_i / k_B T_H} \tag{1.37}$$

with $E_0 = -13.6 \, \text{eV} \equiv -E_i$, where E_i is the ionization energy.

Let Z be the total partition function of the system (do not mix with Z for the atomic number) consisting of $N_e \equiv N_p$ free electrons (and protons) out of $N = N_H + N_p$ atoms in a given ensemble. For indistinguishable particles, we have

$$Z\left(V, T, N_e, N_p, N_H\right) = \frac{Z_e^{N_e}}{N_e!} \frac{Z_p^{N_p}}{N_p!} \frac{Z_H^{N_H}}{N_H!} \; . \tag{1.38}$$

From here, we get the free energy

$$F = -k_B T \ln Z \; . \tag{1.39}$$

The actual particle densities which are realized in nature are the ones that give a minimum of the free energy.

To find the most probable state, we should differentiate Eq. (1.39). For large numbers N, we use the Stirling formula

$$\ln N! \approx N \ln N - N \; , \tag{1.40}$$

leading to

$$\begin{aligned} -\frac{F}{k_B T} \approx \; & N_e \ln Z_e + N_p \ln Z_p + N_H \ln Z_H - N_e \ln N_e \\ & + N_e - N_p \ln N_p + N_p - N_H \ln N_H + N_H \; . \end{aligned} \tag{1.41}$$

Making use of $N_H = N - N_p$ and $N_p = N_e$, we find from the vanishing of the derivative

$$\frac{\partial F}{\partial N_e} \sim \ln Z_e + \ln Z_p - \ln Z_H - \ln N_e - \ln N_e + \ln(N - N_e) = 0 \; . \tag{1.42}$$

This results into

$$\frac{Z_e Z_p}{Z_H} = \frac{N_e^2}{N - N_e} \,. \tag{1.43}$$

With the expressions for the partition functions and $m_H \approx m_p$, we arrive at

$$\frac{V}{h^3} (2\pi m_e k_B T)^{3/2} \, e^{-E_i/k_B T} = \frac{N_e^2}{N - N_e} \,. \tag{1.44}$$

Introducing particle densities $N_e/V = n_e$, $N_p/V = n_p$, and $N_H/V = n_H \equiv n_n$, the Saha (equilibrium) equation can be written in the form

$$\begin{aligned} \frac{n_i n_e}{n_n} &= \frac{2g_1}{g_0} \left(\frac{m_e}{2\pi}\right)^{3/2} \hbar^{-3} (k_B T_e)^{3/2} e^{-E_i/k_B T_e} \equiv K(T_e) \\ &\approx 2.4 \times 10^{15} \, (T_e \, [\mathrm{K}])^{3/2} \, e^{-E_i/(T_e \, [\mathrm{eV}])} \quad [\mathrm{cm}^{-3}] \\ &\approx 3 \times 10^{21} \, (T_e \, [\mathrm{eV}])^{3/2} \, e^{-E_i/\left(T_e \, [\mathrm{eV}]\right)} \quad \left[\mathrm{cm}^{-3}\right] \,. \end{aligned} \tag{1.45}$$

Once again, n_e is the electron density, n_n is the neutral particle (hydrogen) density, n_i is the density of single ionized particles (protons), g_ν is the statistical weight ($g_1 = 2$ for electrons and protons, $g_0 = 4$ for hydrogen), $k_B = 1.3807 \times 10^{-16}$ erg/K is the Boltzmann constant, T_e is the electron temperature, m_e is the electron mass, and $E_i = 13.6\,\mathrm{eV}$ is the ionization energy. $1\,\mathrm{eV} \mathrel{\hat{=}} 1.6022 \times 10^{-12}$ erg, $1\,\mathrm{eV} \mathrel{\hat{=}} 1.1605 \times 10^4$ K.

The Saha formula for hydrogen may be written in the form

$$\frac{\alpha_i \alpha_e}{\alpha_n} = \frac{2g_1}{n g_0} \frac{1}{\lambda_e^3} e^{-E_i/k_B T_e} \tag{1.46}$$

where the ionization degrees

$$\alpha_e = \frac{N_e}{N} \,, \quad \alpha_i = \frac{N_i}{N} \,, \quad \alpha_n = \frac{N_H}{N} \,, \tag{1.47}$$

and the thermal de Broglie wavelength

$$\lambda_e = \sqrt{\frac{h^2}{2\pi m_e k_B T}} \tag{1.48}$$

have been introduced. Note that

$$N = N_H + N_i \equiv N_H + N_e \,, \quad N_e \equiv N_i \,, \quad n = \frac{N}{V} \,. \tag{1.49}$$

Thus, the Saha equation determines the degree of ionization in terms of $T \equiv T_e$ and n. When, besides the temperature T, the pressure p is given, we should use an equation of state, that is,

$$p\,V = \sum_\mu N_\mu k_B T_\mu = (1 + \alpha_e)\, N k_B T \,. \tag{1.50}$$

We can then replace

$$n = \frac{p}{(1+\alpha_e)\, k_B T} \,, \tag{1.51}$$

leading to

$$\frac{\alpha_i \alpha_e}{\alpha_n (1+\alpha_e)} = \frac{2g_1}{g_0} \frac{k_B T}{p\lambda_e^3} e^{-E_i/k_B T_e} \,. \tag{1.52}$$

Noting

$$\alpha_n \equiv \alpha_H = 1 - \alpha_e \,, \quad \alpha_i \equiv \alpha_e \tag{1.53}$$

for hydrogen, we may write

$$\frac{\alpha_e^2}{(1-\alpha_e)(1+\alpha_e)} = \frac{k_B T}{p\lambda_e^3} e^{-E_i/k_B T} \equiv \frac{1}{p\mathcal{K}_p(T)} \,. \tag{1.54}$$

The solution of this quadratic equation is

$$\alpha_e = \frac{1}{\sqrt{1 + p\mathcal{K}_p(T)}} \,, \quad \mathcal{K}_p(T) = \frac{\lambda_e^3}{k_B T} e^{E_i/k_B T} \,. \tag{1.55}$$

This formula allows one to determine the degree of ionization α_e for a given gas pressure p as a function of temperature T. The numerical evaluation is straightforward. Note

$$\begin{aligned} m_e &\approx 9.109 \times 10^{-31}\,\mathrm{kg} \,, & h &\approx 6.626 \times 10^{-34}\,\mathrm{J\,s} \\ 1\,\mathrm{eV} &\approx 1.602 \times 10^{-19}\,\mathrm{J} \,, & 1\,\mathrm{bar} &= 10^5\,\mathrm{N/m^2} \\ E_i &\approx 13.6057\,\mathrm{eV} \,, & k_B &\approx 1.3807 \times 10^{-16}\,\mathrm{erg/deg(K)} \,. \end{aligned}$$

In a similar way, one can derive the degree of ionization for a prescribed total density $n = N/V$ by

$$\alpha_e = \frac{1}{2n\mathcal{K}_n(T)} \left[\sqrt{1 + 4n\mathcal{K}_n(T)} - 1\right], \quad \mathcal{K}_n(T) = \frac{\mathcal{K}_p(T)}{k_B T} \,. \tag{1.56}$$

The dependence of n_i/n_n on temperature for a fixed pressure p is shown in Figure 1.1. Another form of the Saha equation starts from the partition functions Z_i and Z_{i+1} for the atom in its initial and final stages of ionization. The ratio of the number of atoms in stage $i+1$ to the number of atoms in stage i is

$$\frac{N_{i+1}}{N_i} = \frac{2Z_{i+1}}{n_e Z_i} \left(\frac{2\pi m_e k_B T}{h^2}\right)^{3/2} e^{-\chi_i/k_B T} \,, \tag{1.57}$$

where χ_i is the ionization energy needed to remove an electron from ionization stage i to $i+1$. Because a free electron is produced in the ionization process, the number density of free electrons appears on the right-hand side. As n_e increases,

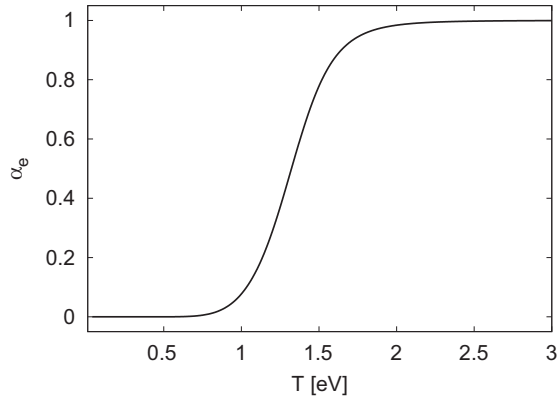

Figure 1.1 Evaluation of the Saha equation (1.55) for hydrogen ($E_i = 13.6\,\text{eV}$) with pressure $p = 1\,\text{bar}$.

the number of atoms in the higher stage of ionization decreases since there are more electrons with which the ion may recombine. Sometimes, the abbreviated form

$$\frac{Z_i}{N_i} = \frac{Z_{i+1} Z_e}{N_{i+1} N_e} \tag{1.58}$$

is said to be the most useful form. Convince yourself that all forms presented here are equivalent.

The Saha equation can also be seen as a restatement of the equilibrium condition for the chemical potentials (note the definition of the chemical potential in terms of a derivative of the free energy and compare with the previous derivation of the most probable state),

$$\mu_i = \mu_{i+1} + \mu_e \,. \tag{1.59}$$

This equation states that the potential of an atom of ionization state i to ionize is the same as the sum of the potentials of an electron and an atom of ionization state $i + 1$. The potentials are equal and therefore the system is in equilibrium and no net change of ionization will occur.

The Saha equation named after the Indian astrophysicist Meghnad Saha who first derived it in 1920 [28].

1.2.2 Thomson Cross Section and Rate Equation

The cross section for the collisional ionization process can be easily estimated. The following estimate treats the collision process on the atomic scale (Bohr radius) in a (in principle not valid) classical model. Nevertheless, the results are close to the exact quantum-mechanical calculation.

When an electron approaches an H-atom on atomic dimension, we consider the scattering from the nucleus. Let us assume large velocities such that the scattering angle is small. The electron is accelerated in the Coulomb field of a proton. If ρ is the transverse distance being approximated by the *constant* scattering parameter ρ, the strength of the force is approximately proportional to $e^2/(\rho^2 + v_e^2 t^2)$, where v_e is the characteristic velocity. The closest approach is at $t = 0$. The perpendicular component requires an additional factor, which is one for the closest approach and decays approximately as $\rho/(\rho^2 + v_e^2 t^2)^{1/2}$ for larger t. Thus, the transverse (to the initial velocity) velocity change is

$$\frac{dv_\perp}{dt} \approx \frac{1}{4\pi\varepsilon_0}\frac{e^2}{m_e}\frac{\rho}{\left(\rho^2 + v_e^2 t^2\right)^{3/2}} \,. \tag{1.60}$$

Figure 1.2 shows some definitions of angles during the scattering, where θ is called the scattering angle, and α has been introduced to calculate the perpendicular component of the Coulomb force. The velocity of the electron is $v \mathrel{\hat{=}} v_e$. Integrating, we get the perpendicular velocity

$$v_\perp \approx \frac{1}{4\pi\varepsilon_0}\frac{e^2}{m_e}\int_{-\infty}^{\infty}\frac{\rho}{\left(\rho^2 + v_e^2 t^2\right)^{3/2}}dt = \frac{1}{4\pi\varepsilon_0}\frac{2e^2}{m_e v_e \rho} \,. \tag{1.61}$$

The energy difference

$$\Delta E_\perp \equiv \frac{m_e v_\perp^2}{2} \approx \frac{1}{(4\pi\varepsilon_0)^2}\frac{e^4}{E\rho^2} \equiv \varepsilon \,, \quad E = \frac{m_e v_e^2}{2} \,, \tag{1.62}$$

is available for collisional ionization. Rewriting the last relation as

$$\rho^2 = \frac{1}{(4\pi\varepsilon_0)^2}\frac{e^4}{E\varepsilon} \,, \tag{1.63}$$

we obtain the relation between collision parameter ρ, initial energy E, and energy change ε. The differential cross section for an energy change $d\varepsilon$ for given initial energy E is

$$d\sigma = |2\pi\rho d\rho| = \frac{1}{(4\pi\varepsilon_0)^2}\frac{\pi e^4}{E\varepsilon^2}d\varepsilon \,. \tag{1.64}$$

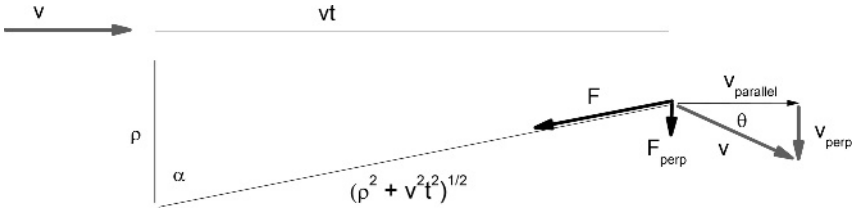

Figure 1.2 The velocity $\boldsymbol{v}$ of an electron approaching a proton at collision parameter ρ at two instances of time. On the left the velocity at $t = -\infty$ is shown. At a later time t, scattering occurred with scattering angle θ. $\boldsymbol{F}$ designates the electrostatic force between the electron and the proton at time t.

The hydrogen atom will be ionized if $\varepsilon > E_i$, where E_i is the ionization energy. Integrating from E_i to E, we obtain the Thomson cross section

$$\sigma_T = \frac{1}{(4\pi\varepsilon_0)^2}\frac{\pi e^4}{E^2 E_i}(E - E_i) \,. \tag{1.65}$$

The maximum cross section occurs for $E = 2E_i$. It is

$$\sigma_{T,max} = \frac{1}{(4\pi\varepsilon_0)^2}\frac{\pi e^4}{4E_i^2} \approx \pi a_B^2 \approx 10^{-16}\,\mathrm{cm}^2 \,, \tag{1.66}$$

where a_B is the Bohr radius. The latter is given by

$$a_B = \frac{4\pi\varepsilon_0\hbar^2}{m_e e^2} \approx 0.529 \times 10^{-10}\,\mathrm{m} \,, \tag{1.67}$$

and the ionization energy is

$$E_i = \frac{m_e e^4}{8\varepsilon_0^2 h^2} \,. \tag{1.68}$$

At large energies, the cross section decays proportional to $1/E$. More exact quantum calculations lead to a decay proportional to $\ln(E)/E$ for $E \gg E_i$ which better agrees with experiments.

Multiplying the cross section with the velocity and the density of scatterers, we obtain the probability of collisional ionization per time. Totally, the change is also proportional to the density of incident particles. For *collisional ionization* and (triple) recombination, the electron particle balance is then

$$\frac{dn_e}{dt} = n_e n_H \langle\sigma_T v_e\rangle - \beta n_e^2 n_p \,, \tag{1.69}$$

where we abbreviate $\langle\sigma_T v_e\rangle \equiv \alpha$ for the mean product of cross section with velocity. The recombination coefficient β can be found in the stationary state from

$$\beta = \frac{n_H\langle\sigma_T v_e\rangle}{n_e n_p} \equiv \frac{\alpha}{K(T)} \,, \tag{1.70}$$

where in the last reformulation, we used the Saha equation; $K(T)$ is on the right-hand side of the Saha formula.

1.2.3 The Corona Formula

When investigating all possible mechanisms for ionization and recombination in a plasma, a modified ionization formula is often used for the intermediate range of electron temperature and density which is of interest for laboratory experiments and astrophysics. That formula portrays, under certain situations, the physical phenomena better than previous calculations. In some hydrogen discharges, it may

yield the tenfold value for the neutral plasma component, as would be expected from the Saha equation.

Let us give some arguments why, besides collisional ionization, other processes are sometimes important. Thus far, we considered collisional ionization, for example, of hydrogen. The process is

$$\mathrm{H} + \mathrm{e}^- \rightarrow \mathrm{H}^+ + \mathrm{e}^- + \mathrm{e}^- \tag{1.71}$$

The inverse process is (triple) recombination

$$\mathrm{H}^+ + \mathrm{e}^- + \mathrm{e}^- \rightarrow \mathrm{H} + \mathrm{e}^- \tag{1.72}$$

The Saha equation covers these processes in thermodynamic equilibrium.

Another ionization and recombination channel is *photoionization*

$$\mathrm{H} + \hbar\omega \rightarrow \mathrm{H}^+ + \mathrm{e}^- \tag{1.73}$$

and photorecombination

$$\mathrm{H}^+ + \mathrm{e}^- \rightarrow \mathrm{H} + \hbar\omega \tag{1.74}$$

We can combine all these processes in the rate equation

$$\frac{dn_e}{dt} = \alpha n_e n_H - \beta n_e^2 n_p + \mu n_H - \gamma n_e n_p \ , \tag{1.75}$$

with coefficients α (collisional ionization from the ground state), β (collisional three-body recombination), μ (photoionization), and γ (electron–ion radiative recombination), respectively. At thermal equilibrium, assuming a detailed balance, we should have

$$\mu = \gamma \frac{n_e n_p}{n_H} \equiv \gamma K(T) \ . \tag{1.76}$$

Under laboratory conditions, the radiation can often leave the plasma. That is why the photon density can be much lower than in equilibrium. For this reason, one can often neglect the photoionization. When the plasma is rarefied, one can also neglect the triple recombination. The corresponding condition is

$$\frac{\mu}{\alpha} \ll n_e \ll \frac{\gamma}{\beta} \ . \tag{1.77}$$

In this limit, the equilibrium electron concentration is given by the balance between photorecombination and collisional ionization, and we arrive at the Elwert formula

$$\frac{n_p}{n_H} = \frac{\alpha}{\gamma} \ . \tag{1.78}$$

This relation is also called the corona equilibrium formula. In many astrophysical situations, this balance is appropriate. The corona model is usually assumed to be applicable if [29]

$$10^{12} t_I^{-1} < n_e \left[\mathrm{cm}^{-3}\right] < 10^{16} T_e \, [\mathrm{eV}]^{7/2} \ , \tag{1.79}$$

where t_I is the normalized ionization time.

For the γ-coefficient, we may use the formula [30]

$$\gamma \approx 2.7 \times 10^{-13}\, T_e^{-1/2} \left[\frac{\mathrm{cm}^3}{\mathrm{s}}\right] \quad \text{when} \quad 1 < T_e\,[\mathrm{eV}] < 15\ . \tag{1.80}$$

Collisional three-body recombination is often approximated by [29]

$$\beta \approx 8.75 \times 10^{-27} (T_e\,[\mathrm{eV}])^{-4.5} \left[\frac{\mathrm{cm}^6}{\mathrm{s}}\right]. \tag{1.81}$$

The interested reader is referred to [31] for more details.

1.3 Characteristic Parameters

Temperature and density are two characteristic parameters of plasmas. For the temperature, the attributes hot and cold are, of course, relative. Similar is the situation for the density when we talk about high and low densities. In this section, we want to establish a better understanding for the relevant orders of magnitude.

In magnetic confinement, hot means high temperatures fulfill the Lawson criterion. Then, we are in the temperature range

$$10\,\mathrm{keV} \leq k_B\, T \leq 20\,\mathrm{keV}\ , \tag{1.82}$$

and the Lawson criterion [32] reads[2)]

$$n k_B\, T \tau_E \geq 3 \times 10^{21}\ \mathrm{m}^{-3}\,\mathrm{keV\,s}\ . \tag{1.83}$$

Here, τ_E is the energy confinement time.

The first question we want to deal with is whether a *relativistic* treatment is required. As a rough estimate for the need of a relativistic treatment, we postulate

$$\frac{v_{the}^2}{c^2} \geq 0.01\ , \tag{1.84}$$

with the electron thermal velocity

$$v_{the} = \left(\frac{k_B\, T_e}{m_e}\right)^{1/2}\ . \tag{1.85}$$

It is straightforward to find the temperature range for the necessity of a relativistic treatment in the form

$$k_B\, T_e \geq 0.01\, m_e c^2 \approx 0.005\ \mathrm{MeV} = 5\,\mathrm{keV} \mathrel{\hat{\approx}} 50\,000\,000\ \mathrm{K}\ . \tag{1.86}$$

2) John D. Lawson, an engineer, was noted for his 1955 paper, published in 1957 [32].

Here, we made use of the approximate values

$$m_e c^2 \approx 0.5\,\mathrm{MeV}\,, \quad 1\,\mathrm{eV} \,\hat{\approx}\, 10\,000\,\mathrm{K}\,. \tag{1.87}$$

More exact values can be obtained when using more precise constants; see, for example, [29].

Quantum effects become important when the degeneracy parameter $n_e \lambda_{dB}^3$ becomes larger than one. In the *nonrelativistic* case, we use the thermal de Broglie wavelength

$$\lambda_{dB} \equiv \lambda_e = \frac{h}{\sqrt{2\pi m_e k_B T_e}}\,. \tag{1.88}$$

Then,

$$n_e \gg \left(\frac{m_e k_B T_e}{\hbar^2}\right)^{3/2} \tag{1.89}$$

follows for the need of a quantum-mechanical description.

In the *relativistic* case, we use the energy expression

$$E^2 = c^2 p^2 + m_e^2 c^4 \tag{1.90}$$

together with $E \sim k_B T_e$ as well as $\lambda_{dB} \sim h/p$. In the *ultrarelativistic* case, from $p \sim k_B T_e / c$,

$$n_e \gg \left(\frac{k_B T_e}{\hbar c}\right)^3 \tag{1.91}$$

follows. For the general case Eq. (1.90), the generalization of the estimate Eq. (1.91) is straightforward to obtain. In Figure 1.3, we have plotted the borderline between the classical and the quantum-mechanical behaviors. The areas of applicability of other model zones are also shown.

The *ideal* gas approximation proves to be good if the nonideality parameter $|E_{pot}|/|E_{kin}|$ is small. Since

$$E_{pot} \sim \frac{1}{4\pi\varepsilon_0}\frac{e^2}{\lambda_n} \sim n_e^{1/3} \tag{1.92}$$

and

$$E_{kin} = \frac{3}{2} k_B T_e \quad [\text{classical}]\,, \tag{1.93}$$

we can express, with the electron Debye length $\lambda_{De} = (\varepsilon_0 k_B T_e / n_e e^2)^{1/2}$, the *classical ideality condition* as

$$n_e \lambda_{De}^3 \gg 1\,. \tag{1.94}$$

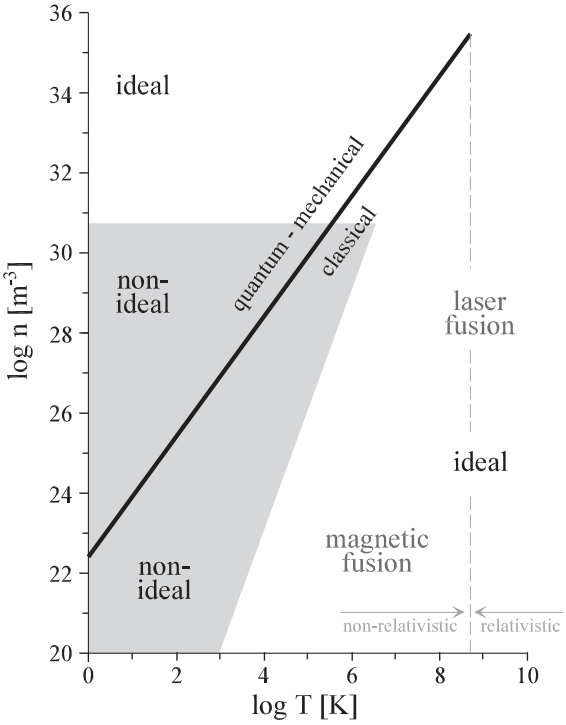

Figure 1.3 Overview over different model approximations in physical parameter space.

When a quantum-mechanical description is appropriate, the estimate is different. Then, we approximate

$$E_{kin} \approx \frac{p_F^2}{2m_e} \sim \frac{h^2 n_e^{2/3}}{m_e} \,, \tag{1.95}$$

with the Fermi momentum p_F to find the *quantum-mechanical ideality condition*

$$\lambda_B \equiv \frac{e^2 m_e}{4\pi\varepsilon_0 n_e^{1/3}\hbar^2} \ll 1 \,. \tag{1.96}$$

The expression λ_B on the left-hand side is called the Brueckner parameter. Note the different conditions for ideality (in terms of the density) in the classical and quantum-mechanical regimes, respectively. In the classical case, we have

$$\frac{E_{Coulomb}}{k_B T_e} \sim n_e^{1/3} \,, \tag{1.97}$$

whereas in the quantum case,

$$\frac{E_{Coulomb}}{\frac{p_F^2}{2m_e}} \sim n_e^{-1/3} \tag{1.98}$$

follows.

A global overview over different model approximations in physical parameter space is shown in Figure 1.3.

We conclude this subsection by the quite surprising remark that "low" temperatures in quantum-mechanically degenerate systems, that is,

$$k_B T_e \ll \varepsilon_F \equiv \sqrt{m_e^2 c^4 + c^2 p_F^2}\,, \tag{1.99}$$

may be extremely "high", in the sense that relativistic effects are important. The latter appear for

$$p_F > m_e c \tag{1.100}$$

with

$$p_F = \left(\frac{3n_e}{8\pi}\right)^{1/3} h\,. \tag{1.101}$$

Thus, for

$$n_e \gg \left(\frac{m_e c}{h}\right)^3, \tag{1.102}$$

we have to perform relativistic calculations even if the temperatures are "low."

In the following, we discuss two important applications in more detail.

1.3.1 Typical Parameters of (Magnetic) Fusion Plasmas

When developing a theory, we have to specify the parameter regime to which it should apply. In the following, we show typical parameters[3] for a magnetic fusion plasma,

$$T \approx 10\,\mathrm{keV}\,, \quad B \approx 4\,\mathrm{T} \mathrel{\hat{=}} 4\times 10^4\,\mathrm{G}\,, \quad n_e \approx n_i := n \approx 10^{14}\,\mathrm{cm}^{-3}\,. \tag{1.103}$$

For these parameters, the Debye length is then of the order

$$\lambda_D \approx 7.43\times 10^2\, T^{1/2} n^{-1/2}\,[\mathrm{cm}] \approx 7\times 10^{-3}\,\mathrm{cm}\,. \tag{1.104}$$

Thermal de Broglie wavelength, mean particle distance and thermal velocity are

$$\lambda_{dB} \approx 2.76\times 10^{-8}\, T^{-1/2}\,[\mathrm{cm}] \approx 3\times 10^{-10}\,\mathrm{cm}\,, \tag{1.105}$$

$$\lambda_n \approx n^{-1/3}\,[\mathrm{cm}] \approx 10^{-5}\,\mathrm{cm}\,, \tag{1.106}$$

$$v_{the} \approx 4.19\times 10^7\, T^{1/2}\left[\frac{\mathrm{cm}}{\mathrm{s}}\right] \approx 4\times 10^9\,\frac{\mathrm{cm}}{\mathrm{s}}\,. \tag{1.107}$$

3) Only within the next few formulas, should B be inserted in gauss units, as it is often done in fusion applications [29]. Thus, when not stated otherwise, in this subsection, T is in electron volt and B in gauss.

Larmor radii follow via the gyrofrequency $\Omega = qB/m$ (in SI units) divided by the thermal velocity,

$$\rho_i \approx 1.02 \times 10^2 \, T_i^{1/2} \, B^{-1} \, [\mathrm{cm}] \approx 0.2 \, \mathrm{cm} \, , \tag{1.108}$$

$$\rho_e \approx 2.38 \, T_e^{1/2} \, B^{-1} \, [\mathrm{cm}] \approx 0.5 \times 10^{-2} \, \mathrm{cm} \, . \tag{1.109}$$

A plasma is magnetized for $\delta \equiv \rho / L \ll 1$, that is,

$$\delta_i \approx \sqrt{\frac{m_i}{m_e}} \delta_e \ll 1 \, . \tag{1.110}$$

The total collision cross section $\sigma_{tot} \equiv \pi R^2$ (see previous and following discussions) is often estimated by making use of

$$\frac{1}{4\pi\varepsilon_0} \frac{e^2}{R} \approx T \, . \tag{1.111}$$

Then, the mean free path of a particle

$$\lambda_{mfp} \sim v_{th} \nu^{-1} \sim \frac{1}{\sigma_{tot} n} \quad [\text{estimate}] \tag{1.112}$$

turns out to vary as

$$\lambda_{mfp} \sim \frac{T^2}{n} \, . \tag{1.113}$$

The more exact formula [29] leads, for example for electrons, to

$$\lambda_{mfp} \approx 10^6 \, \mathrm{cm} \, . \tag{1.114}$$

From the mean free paths, estimates of the collision frequencies also follow. Here, we present the kinetic collision frequencies $\nu \sim \lambda_{mfp} / v_{th}$ as

$$\nu_e \approx 2.91 \times 10^{-6} \, n_e \ln \Lambda \, T_e^{-3/2} \left[\mathrm{s}^{-1} \right] \approx 3 \times 10^3 \, \mathrm{s}^{-1} \, , \tag{1.115}$$

$$\nu_i \approx 4.78 \times 10^{-8} \, n_i \ln \Lambda \, T_i^{-3/2} \left[\mathrm{s}^{-1} \right] \approx 5 \times 10^1 \, \mathrm{s}^{-1} \, , \tag{1.116}$$

where $\ln \Lambda$ is the Coulomb logarithm (see later chapters). The gyrofrequencies have the orders of magnitude

$$|\Omega_e| \approx 1.76 \times 10^7 \, B \left[\frac{\mathrm{rad}}{\mathrm{s}} \right] \approx 8 \times 10^{11} \, \frac{\mathrm{rad}}{\mathrm{s}} \, , \tag{1.117}$$

$$\Omega_i \approx 9.58 \times 10^3 \frac{\mathrm{rad}}{\mathrm{s}} \sim 4 \times 10^8 \, \frac{\mathrm{rad}}{\mathrm{s}} \, . \tag{1.118}$$

In a plasma, a collective electron plasma frequency also appears,

$$\omega_{pe} = \sqrt{\frac{n e^2}{\varepsilon_0 m_e}} \sim 5.64 \times 10^4 \, n_e^{1/2} \left[\frac{\mathrm{rad}}{\mathrm{s}} \right] \approx 5 \times 10^{11} \frac{\mathrm{rad}}{\mathrm{s}} \, . \tag{1.119}$$

Similarly, an ion plasma frequency exists, that is,

$$\omega_{pi} \approx 1.32 \times 10^3 \, n_i^{1/2} \left[\frac{\mathrm{rad}}{\mathrm{s}} \right] \approx 10^{10} \, \frac{\mathrm{rad}}{\mathrm{s}} \, . \tag{1.120}$$

1.3.2 Parameters of the Sun

In our opinion, the most important burning star is the sun which provides us with the necessary energy for life. Thermonuclear fusion in gravitational confinement is its energy source. Geological observations do not show any indications for significant changes in the behavior of the sun during the last million years. Thus, we may assume that the sun is in hydrostatic equilibrium. The gravitational energy can be estimated by (we assume an approximately constant mass density $\rho = \text{const}$)

$$E_{Gr} = -\int_0^R \frac{G\,m(r)\rho(r)}{r} 4\pi r^2 dr$$
$$= -\frac{(4\pi)^2}{3} G\rho^2 \int_0^R r^4 dr = -\frac{3}{5}\frac{G\,M^2}{R} \sim \mathcal{O}\left(-\frac{G\,M^2}{R}\right) . \tag{1.121}$$

Here, $m(r)$ is the mass of the sphere up to radius r; it is the "enclosed mass." In the following, we shall use

$$E_{Gr} \approx -\frac{G\,M_\odot^2}{R_\odot} . \tag{1.122}$$

The exact numerical factors are not needed for a rough estimate. In Eq. (1.122), $R_\odot$ is the radius and $M_\odot$ is the mass of the sun. Astrophysical observations provide us with the values $M_\odot = 1.99 \times 10^{30}$ kg and $R_\odot = 6.96 \times 10^8$ m. The age of the sun is estimated as $t_\odot \approx 4.55$ Gyr. Measurements of the luminosity $L_\odot$ deliver the basis for estimates of the surface temperature $T_\odot$. The approximate value for the luminosity is $L_\odot = 3.86 \times 10^{26}$ W. Making use of the luminosity formula $L_\odot = 4\pi R_\odot^2 \sigma T_O^4$ with the Stefan–Boltzmann constant σ, we find for the surface temperature $T_O \approx T_\odot \equiv 5780 \approx 6000$ K. This value is quite different from the temperature in the interior of the sun. The latter should be much larger in order to enable the nuclear fusion process.

The physical parameters of the interior of the sun follow from solar models [18, 19]. Solar models are meanwhile quite advanced. Typical values for the central temperature, central mass density, and pressure at the center, respectively, are

$$T_c = 15.6 \times 10^6 \text{ K} , \tag{1.123}$$

$$\rho_c = 1.48 \times 10^5 \text{ kg m}^{-3} , \tag{1.124}$$

$$P_c = 2.29 \times 10^{16} \text{ Pa} . \tag{1.125}$$

The large central temperature becomes plausible from the following estimate based on the stationarity condition

$$\frac{dP}{dr} = -\rho \frac{G\,M_r}{r^2} , \tag{1.126}$$

where $M_r \equiv m(r)$ is the "enclosed mass," G the gravitational constant, and P is the pressure. This is a minimal model; many effects are neglected.

Multiplying Eq. (1.126) by $4\pi r^3$ and integrating over r from zero to $R \approx R_\odot$ leads to

$$\int_0^R dr 4\pi r^3 \frac{dP}{dr} = -\int \frac{G M_r}{r} dm \equiv E_{Gr} , \tag{1.127}$$

with $dm = 4\pi r^2 \rho dr$. E_{Gr} is the potential (gravitational) energy of the whole mass distribution and ρ is the mass density.

Next, we integrate on the left-hand side by parts. For (nearly) vanishing pressure at the surface $R \approx R_\odot$, we obtain

$$-3\langle P \rangle V = E_{Gr} , \tag{1.128}$$

with the averaged pressure

$$\langle P \rangle = \frac{\int P(r) dV}{\int dV} . \tag{1.129}$$

The averaged pressure is the mean pressure value averaged over the whole volume. With the new notation, Eq. (1.128) is known as the virial theorem, usually written in the form

$$\langle P \rangle = -\frac{1}{3} \frac{E_{Gr}}{V}. \tag{1.130}$$

The contents of the virial theorem is the maximum information we can get without specifying an equation of state.

Making use of the virial theorem, we find for the sun $\langle P \rangle \approx 10^{14}$ Pa. Note that we obtain the mean pressure averaged over the whole volume. The pressure in the center is much larger. When we are interested in more details, we need the equation of state. For rough values, a classical calculation is still possible. In addition, although deviations from the ideal gas law will become significant, for simplicity, we still use the ideal gas approximation

$$\langle P \rangle = nkT = \frac{\langle \rho \rangle}{\bar{m}} kT . \tag{1.131}$$

This leads to the mean temperature for the hydrostatic equilibrium $\langle T \rangle \approx 6 \times 10^6$ K. That temperature is much larger than the surface temperature (by a factor of approx. 10^3), and reasonably close to the temperature at center $T_c \approx 15.6 \times 10^6$ K. In any case, the low surface temperature is very important. Larger surface temperatures would lead to a X-ray bombardment on the earth, making life in its present form impossible.

1.4 Individual and Collective Effects

In this section, we discuss the differences between individual and collective effects in more detail. We have already mentioned that binary collisions are typical indi-

vidual effects. Their strength is measured in terms of a collision frequency ν. The latter should be compared with the plasma frequency ω_p, a typical collective phenomenon. Let us now first work out the physical meaning of the electron plasma frequency ω_{pe}.

1.4.1 The Plasma Frequency

A "Gedankenexperiment" starts from a sphere of radius r uniformly filled with electrons and protons such that the whole system is globally neutral. If, on the other hand, only one species, for example, electrons, would be present, the sphere would have a charge q_e resulting in a radial field at the surface,

$$q_e = -\frac{4\pi}{3} r^3 e n_e \,, \quad |E| = \frac{1}{4\pi\varepsilon_0}\frac{q_e}{r^2} \,. \tag{1.132}$$

The field strength could be enormously large, depending on the size of the sphere and the electron density. However, as stated already, we start our "Gedankenexperiment" with homogeneously distributed electrons and protons such that outside the sphere no electric field exists. Next, let us expand the electron sphere from radius r to radius $r + x$ with $x \ll r$, creating an electron shell of thickness x. Since the total number N of electrons and protons, respectively, is constant, the electron density is decreased to

$$n_e = n_{e0} + \delta n_e \approx \frac{N}{\frac{4\pi}{3} r^3 \left(1 + 3\frac{x}{r}\right)} \approx n_{e0} - 3 n_{e0}\frac{x}{r} \,. \tag{1.133}$$

Within the sphere of radius r, we now have a positive excess charge

$$\Delta q \approx 4\pi n_{e0} e r^2 x, \tag{1.134}$$

creating, at r, the radial electric field component

$$E \approx \frac{1}{4\pi\varepsilon_0} 4\pi e n_{e0} x \,. \tag{1.135}$$

A shell electron feels the radial force

$$K \equiv m_e \frac{d^2x}{dt^2} = -eE = -\frac{1}{\varepsilon_0} e^2 n_{e0} x \,, \tag{1.136}$$

which pulls it back into the original sphere. An overshooting will occur, resulting in oscillations with the electron plasma frequency

$$\omega_{pe} = \sqrt{\frac{e^2 n_e}{\varepsilon_0 m_e}} \,. \tag{1.137}$$

In this scenario, we kept the ions fixed, having in mind their large mass compared to the electron mass and the high-frequency of the electron oscillations.

The Debye length is connected to the plasma frequency via

$$\lambda_D = \frac{v_{th}}{\omega_p} \,. \tag{1.138}$$

1.4.2
General Remark on Individual Collisions

Next, we will discuss the individual collision frequencies in more detail. Binary collisions correspond to the classical two-body problem. At this point, we should mention that the two-body problem with Coulomb interaction can be reduced to an effective one-particle problem if we go to the center of mass (COM) system. Then, the reduced mass appears. If one mass is much larger than the other (or if we fix the position of the scatterer, which effectively means that we assume an infinitely large mass of the scatterer), the difference between COM and laboratory system disappears. The next considerations can be interpreted as the calculations for a fixed scatterer. The two-body problem with a *fixed scattering center* is depicted in Figure 1.4.

A charge $q = +e$ scatters a beam of electrons with charge $-e$. The incoming particle current density is $j = n_e v_e$. Per time unit, we have $2\pi\rho d\rho j$ particles being scattered when passing through a ring area $2\pi\rho d\rho$. Each particle is scattered at a specific angle θ. Asymptotically, the change of *longitudinal* (i.e., in the direction of initial propagation) momentum of a single particle is

$$\Delta p_0 = -m_e v_e (1 - \cos\theta) \,. \tag{1.139}$$

We can define the total force on the *beam* (in the presence of a fixed scatterer), whose magnitude is

$$F_e = -\int_0^\infty m v_e (1 - \cos\theta)\, j\, 2\pi\rho d\rho \mathrel{\hat{=}} -m_e v_e j\, \sigma \,. \tag{1.140}$$

Here, we assumed fixed initial velocities of magnitude v_e. The expression

$$\sigma = \int_0^\infty (1 - \cos\theta) 2\pi\rho d\rho \tag{1.141}$$

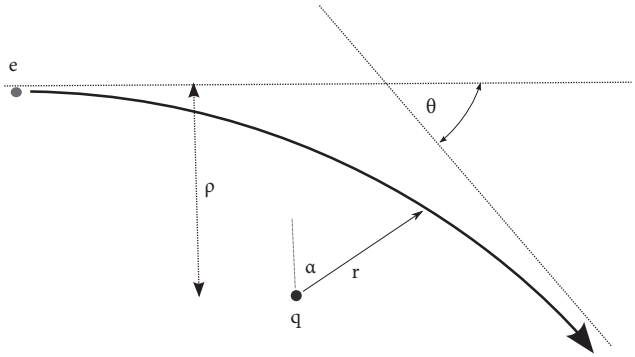

Figure 1.4 Sketch of a two-particle collision.

is called the transport cross section (for momentum transfer). To evaluate the latter, we need the functional dependence $\theta = \theta(\rho)$. That can be taken from standard textbooks of classical mechanics [33],

$$\tan\frac{\theta}{2} = \frac{1}{4\pi\varepsilon_0}\frac{e^2}{m_e\rho v_e^2}\,. \tag{1.142}$$

As a side note, this relation can be made easily plausible for small scattering angles $\theta \ll 1$. Then, the straight-path approximation may be assumed in evaluating integrals. For example, we get for the transverse momentum change

$$\begin{aligned}\Delta p_{0\perp} \approx m_e v_e \theta &= \int_{-\infty}^{\infty} F_\perp\, dt \approx \frac{1}{4\pi\varepsilon_0}\int_{-\infty}^{\infty}\frac{e^2\rho}{\left(\rho^2 + v_e^2 t^2\right)^{3/2}}\,dt \\ &= \frac{1}{4\pi\varepsilon_0}\frac{2e^2}{\rho v_e}\,,\end{aligned} \tag{1.143}$$

where we have approximated $\sin\theta \approx \theta$ and $\cos\alpha \approx \rho/\sqrt{\rho^2 + v_e^2 t^2}$. The angle θ is the scattering angle and α is the angle between the total force and the perpendicular component.

Evaluating the cross section Eq. (1.141), we make us of $1 - \cos\theta \approx \theta^2/2$ to obtain

$$\sigma = \frac{1}{(4\pi\varepsilon_0)^2}\frac{4\pi e^4}{m_e^2 v_e^4}\int_0^{\infty}\frac{1}{\rho}\,d\rho\,. \tag{1.144}$$

Apparently, the integral is logarithmically divergent. As a lower limit, we define

$$\rho_{min} = \frac{1}{4\pi\varepsilon_0}\frac{e^2}{m_e v_e^2}\,, \tag{1.145}$$

which is the collision parameter for 90° scattering. Note that $\tan(\pi/4) = 1$. For more details, see the chapter on transport theory. For very small collision parameters (strong collisions), a classical treatment will break down. The upper limit $\rho_{max} = \lambda_D$ is postulated as the Debye length due to the screening of the potential of the scatterer. Thus, we evaluate, instead of Eq. (1.144),

$$\sigma = \frac{1}{(4\pi\varepsilon_0)^2}\frac{4\pi e^4}{m_e^2 v_e^4}\int_{\rho_{min}}^{\rho_{max}}\frac{1}{\rho}\,d\rho\,. \tag{1.146}$$

The expression

$$\ln\Lambda = \ln\frac{\rho_{max}}{\rho_{min}} = \ln 16\pi^2\varepsilon_0^{5/2}\frac{3(k_B T)^{3/2}}{e^3\sqrt{n}} \tag{1.147}$$

is proportional to the logarithm of the number of particles in the Debye sphere and is called the Coulomb logarithm. In magnetic fusion plasmas, it is of the order 10–20. In Eq. (1.147), we have used

$$\frac{1}{2}m_e v_e^2 \approx \frac{3}{2}k_B T\,. \tag{1.148}$$

Of course, within an approximate treatment, also slightly different estimates are in use. The result for the cross section is now

$$\sigma = \frac{1}{(4\pi\varepsilon_0)^2}\frac{4\pi e^4}{m_e^2 v_e^4}\ln\Lambda \ . \tag{1.149}$$

We find the order of magnitude

$$\sigma \sim \frac{10^{-12}}{(E\,[\mathrm{eV}])^2}\,\mathrm{cm}^2 \ , \tag{1.150}$$

where $E = 1/2\, m_e v_e^2$ is the kinetic energy.

1.4.3 Collision Frequencies for Momentum and Energy Transfer

The transport cross section allows us to find the *momentum* transfer rate between particles. Let us consider an electron beam in a cold plasma. Then, we still assume the scatterers as fixed. Let n_i be the ion density. When we have n_i scatterers per unit volume, the mean force acting on a single particle of the beam will be

$$\boldsymbol{F}_e = -m_e \boldsymbol{v}_e\, j\, \sigma n_i \frac{1}{n_e} = -m_e v_e \sigma n_i \boldsymbol{v}_e \ . \tag{1.151}$$

Due to this force, the electron mean velocity is decelerated,

$$\frac{d\boldsymbol{v}_e}{dt} = \frac{\boldsymbol{F}_e}{m_e} = -n_i \sigma v_e \boldsymbol{v}_e \equiv -\nu_{ei}\boldsymbol{v}_e \ . \tag{1.152}$$

Here, $\boldsymbol{v}_e$ is the relative velocity between electron and ion. For a fixed scatterer, the total energy of an electron does not change. The longitudinal velocity component of the scattered electron changes according to Eq. (1.139), or approximately as

$$\Delta v_e = -v_e(1-\cos\theta) \approx -v_e\frac{\theta^2}{2} \ . \tag{1.153}$$

Thus, the angular spread grows, that is,

$$\frac{d\theta^2}{dt} = 2\sigma n_i v_e \ . \tag{1.154}$$

The characteristic time

$$\tau_{ei} = \frac{1}{n_i \sigma v_e} \equiv \frac{1}{\nu_{ei}} \tag{1.155}$$

is the inverse of the collision frequency ν_{ei}.

The collision frequency follows from the cross section after multiplying $n_i v_e$, that is, we obtain the approximate result

$$\nu_{ei} = \frac{1}{(4\pi\varepsilon_0)^2}\frac{4\pi e^4 n_i}{m_e^2 v_e^3}\ln\Lambda \ . \tag{1.156}$$

The ratio between the individual collision frequency and the collective plasma frequency is proportional to the inverse of the number of particles in a Debye sphere,

$$\frac{\nu_{ei}}{\omega_{pe}} \sim \frac{1}{n\lambda_{De}^3} \tag{1.157}$$

for $n_i \approx n_e \approx n$.

Note that after the time $T \approx \nu_{ei}^{-1}$ the quantity θ^2 suffers a change of its order of magnitude. We may calculate characteristic values from

$$\nu_{ei} \sim 6 \times 10^{-5} \frac{n_i\,[\mathrm{cm}^{-3}]}{(E\,[\mathrm{eV}])^{3/2}}\ . \tag{1.158}$$

The electron mean free path is

$$\lambda_{mfpe} = \frac{1}{n_i \sigma} \sim 10^{12} \frac{(E\,[\mathrm{eV}])^2}{n_i\,[\mathrm{cm}^{-3}]}\,\mathrm{cm}\ . \tag{1.159}$$

For a Maxwellian, we may use

$$\langle E^2 \rangle = \frac{15}{4}(k_B\,T)^2\ . \tag{1.160}$$

With that, we determine the temperature dependencies of the characteristic quantities. Measuring lengths in cm, densities in cm^{-3}, and temperatures in eV, we obtain the characteristic values

$$\sigma \sim \frac{3 \times 10^{-13}}{T^2}\,\mathrm{cm}^2\ , \tag{1.161}$$

$$\nu_{ei} \sim 3 \times 10^{-5} \frac{n}{T^{3/2}}\,\mathrm{s}^{-1}\ , \tag{1.162}$$

$$\lambda_{mfpe} \sim 3 \times 10^{12} \frac{T^2}{n}\,\mathrm{cm}\ . \tag{1.163}$$

1.4.3.1 Calculation in the Center of Mass System

When the masses of scatterer (m_2) and scattered particle (m_1) are similar or $m_1 \gg m_2$, we transform to the center of mass system with center of gravity $\boldsymbol{R}$. Using $\boldsymbol{r} = \boldsymbol{r}_2 - \boldsymbol{r}_1$ for the difference of the position vectors, and the reduced mass $m_{12} = m_1 m_2/(m_1 + m_2)$, we have

$$\boldsymbol{r}_1 = \boldsymbol{R} - \frac{m_2}{m_1 + m_2}\boldsymbol{r}\ , \quad \boldsymbol{r}_2 = \boldsymbol{R} + \frac{m_1}{m_1 + m_2}\boldsymbol{r}\ , \tag{1.164}$$

and find

$$m_{12}\ddot{\boldsymbol{r}} = -Z_1 Z_2 e^2 \frac{\boldsymbol{r}}{r^3}\ . \tag{1.165}$$

In the following, we assume that the scatterer has charge $Z_2 e$, while for the scattered particle, the charge is $-Z_1 e$. One obtains an effective two-body problem similar to the treatment for fixed scatterers. The mass has to be replaced by the reduced

mass, and the position of the scatterer is replaced by the relative distance. We can immediately translate the previous formulas, for example, Eq. (1.149) can now be written as

$$\sigma = \frac{1}{(4\pi\varepsilon_0)^2}\frac{4\pi Z_1^2 Z_2^2 e^4}{m_{12}^2 v^4}\ln\Lambda\ , \tag{1.166}$$

and the general formula for the collision frequency (to deflect the incident particle by an angle 90° in the presence of n_2 scatterers per unit volume)

$$\nu_{12} = v\sigma n_2 = \frac{1}{(4\pi\varepsilon_0)^2}\frac{4\pi Z_1^2 Z_2^2 e^4 n_2 \ln\Lambda}{m_{12}^2 v^3}\ . \tag{1.167}$$

Note that we calculated the frequency for velocity deflections. Thus, ν_{12} directly gives the frequency for momentum transfer in the center of gravity system. We shall denote the *momentum* scattering frequencies as $\nu_{ee}, \nu_{ii}, \nu_{ei}$, and ν_{ie} for the various possible interactions between species. The reciprocals are denoted by $\tau \sim \nu^{-1}$.

Energy scattering is characterized by the time required for an incident particle to transfer its kinetic energy to the target particle. The energy transfer collision frequencies are denoted by $\nu_{ee}^E, \nu_{ii}^E, \nu_{ei}^E$, and ν_{ie}^E, respectively.

As a typical velocity, we take $v \sim v_{th}$. We reference all collision frequencies to ν_{ee}. Note for the reduced mass $m_{ee} \sim m_e/2 \sim m_e$ and $v \sim T^{1/2}/m_e^{1/2}$ for this case. When we calculate ν_{ei}, we have $m_{ei} \sim m_e$ and $v \sim T^{1/2}/m_e^{1/2}$, that is, (except for a factor two) the same values, and therefore

$$\nu_{ei} \sim \nu_{ee} \tag{1.168}$$

follows.

Next, we consider ν_{ii}. Now, $m_{ii} \sim m_i/2$ and $v \sim T^{1/2}/m_i^{1/2}$, and therefore

$$\nu_{ii} \sim \sqrt{\frac{m_e}{m_i}}\nu_{ee} \tag{1.169}$$

follows. In all cases, the differences between the lab frame and the center of gravity system are tolerable since we ignore factors of order two in the present estimates.

Care is required when calculating ν_{ie}. The transformation into the lab frame is necessary, straightforward, but not immediately obvious. An easier way to estimate ν_{ie} is momentum conservation in lab frame which leads to $m_i\Delta\boldsymbol{v}_i = -m_e\Delta\boldsymbol{v}_e$ where Δ means the change in quantity as a result of the collision. For a head-on collision, we approximately have $\Delta\boldsymbol{v}_e \approx 2\boldsymbol{v}_i$ and therefore $|\Delta\boldsymbol{v}_i|/|\boldsymbol{v}_i| \approx 2m_e/m_i$. Thus, in order to have $|\Delta\boldsymbol{v}_i|/|\boldsymbol{v}_i|$ of order unity, it is necessary to have m_i/m_e collisions. Hence,

$$\nu_{ie} \sim \frac{m_e}{m_i}\nu_{ee}\ . \tag{1.170}$$

Next, we consider *energy* changes. If a moving electron makes a head-on collision with an electron at rest, then the incident electron stops while the originally

standing electron flies off with the same momentum and energy that the incident electron had. From here, we conclude

$$\nu_{ee}^{E} \sim \nu_{ee} \,. \tag{1.171}$$

A similar picture holds for an ion hitting an ion,

$$\nu_{ii}^{E} \sim \nu_{ii} \sim \sqrt{\frac{m_e}{m_i}}\,\nu_{ee} \,. \tag{1.172}$$

Finally, we compare energy changes during electron–ion and ion–electron collisions. The electron momentum change is $-2m_e\boldsymbol{v}_e$ during a collision of an electron with an ion. From conservation of momentum, we find $m_i\boldsymbol{v}_i = 2m_e\boldsymbol{v}_e$. The energy transferred to the ion is $1/2\,m_i v_i^2 = 4(m_e/m_i)m_e v_e^2/2$. An electron has to make m_i/m_e collisions for transferring all its energy to the ions, and hence

$$\nu_{ei}^{E} \sim \frac{m_e}{m_i}\nu_{ee} \,. \tag{1.173}$$

Similarly, during an ion–electron collision, an electron initially at rest will fly off with twice the incident ion velocity. The electron gains energy $1/2\,m_e v_e^2 \sim 2(m_e/m_i)m_i v_i^2$. Again, approximately m_i/m_e collisions are necessary for the ion to transfer all its energy to the electrons, that is,

$$\nu_{ie}^{E} \sim \frac{m_e}{m_i}\nu_{ee} \,. \tag{1.174}$$

These rough estimates have an important consequence, namely, that we may describe – even in nonequilibrium situations – an electron–ion plasma by a two-fluid model. The relaxation to approximate Maxwellians occurs fast in each component (fastest for the electrons), and the exchange between the components occurs on a much slower scale.

1.4.4
Friction Force in Thermal Plasmas

We now consider a thermal *e*–*i*-plasma. The velocity distribution functions are assumed as

$$f_i\left(\boldsymbol{v}'\right) = \left(\frac{m_i}{2\pi T_i}\right)^{3/2} \exp\left(-\frac{m_i\left(\boldsymbol{v}' - \boldsymbol{u}_i\right)^2}{2T_i}\right) \tag{1.175}$$

and

$$f_e\left(\boldsymbol{v}'\right) = \left(\frac{m_e}{2\pi T_e}\right)^{3/2} \exp\left(-\frac{m_e\left(\boldsymbol{v}' - \boldsymbol{u}_e\right)^2}{2T_e}\right). \tag{1.176}$$

The electric current density in this configuration is

$$\boldsymbol{j} = n_i e\boldsymbol{u}_i - n_e e\boldsymbol{u}_e \,. \tag{1.177}$$

It is appropriate to transform into the system of the mean velocity $\boldsymbol{u}_e$ of the electrons and to define the relative velocity

$$\boldsymbol{u}_{rel} = \boldsymbol{u}_i - \boldsymbol{u}_e \equiv \boldsymbol{u} \,. \tag{1.178}$$

The distribution functions in this frame will be

$$f_i(\boldsymbol{v}) = \left(\frac{m_i}{2\pi T_i}\right)^{3/2} \exp\left(-\frac{m_i\,(\boldsymbol{v}-\boldsymbol{u}_{rel})^2}{2T_i}\right) \tag{1.179}$$

and

$$f_e(\boldsymbol{v}) = \left(\frac{m_e}{2\pi T_e}\right)^{3/2} \exp\left(-\frac{m_e v^2}{2T_e}\right). \tag{1.180}$$

Since the ion thermal velocity is much smaller than the electron thermal velocity, the ion velocity distribution is much narrower than the electron distribution function, and the ions can be considered approximately as a monoenergetic beam. When impinging on n_e electrons per unit volume, we calculate the net force on the ions making use of the previous expressions and applying the actio = reactio principle. Using Eq. (1.151), for a moment we go to the system where the ions are at rest, such that the electrons have velocity $\boldsymbol{v}_e - \boldsymbol{u}$. Then, $\boldsymbol{F}_e$ can be used in the form Eq. (1.151). Setting $\boldsymbol{F}_i = -\boldsymbol{F}_e$, we find

$$\boldsymbol{F}_i = -m_e\,|\boldsymbol{u}-\boldsymbol{v}_e|\;\sigma n_e(\boldsymbol{u}-\boldsymbol{v}_e)\;, \tag{1.181}$$

with ($Z_1 = 1, Z_2 = Z$)

$$\sigma \approx \frac{1}{(4\pi\varepsilon_0)^2}\,\frac{4\pi Z^2 e^4}{m_e^2\,|\boldsymbol{u}-\boldsymbol{v}_e|^4}\ln\Lambda\;. \tag{1.182}$$

By the way, similar formulas would hold for a fast electron component in a thermal plasma. Let us assume that we have a fraction of scatterers in a certain velocity domain. Then, we replace

$$n_e \to dn_e = n_e f_e(\boldsymbol{v}')d^3v'\;. \tag{1.183}$$

We rewrite the friction force for dn_e scatterers per unit volume. Having in mind the relative speed $\boldsymbol{u}-\boldsymbol{v}'$ of the scattered particles, we obtain

$$d\boldsymbol{F}_i = -\frac{1}{(4\pi\varepsilon_0)^2}\,\frac{4\pi Z^2\ln\Lambda e^4 n_e}{m_e}\,\frac{\boldsymbol{u}-\boldsymbol{v}'}{|\boldsymbol{u}-\boldsymbol{v}'|^3}\,f_e\left(\boldsymbol{v}'\right)d^3v'\;. \tag{1.184}$$

When averaging over the possible velocities of the scatterers, one has to evaluate the integral

$$\boldsymbol{I} = \int \frac{\boldsymbol{u}-\boldsymbol{v}'}{|\boldsymbol{u}-\boldsymbol{v}'|^3}\,f_e(\boldsymbol{v}')d^3v'\;. \tag{1.185}$$

Its form reminds us of the integral over a charge distribution appearing when solving the Poisson equation [34]. If the distribution function f is isotropic, the integral corresponds to an electric field caused by a spherically symmetric charge distribution with "radius vector" $\boldsymbol{u}$. We know that the radial electric field at distance u is only caused by the charge within the sphere of "radius" u, that is,

$$\boldsymbol{I} = \frac{\boldsymbol{u}}{u^3} \int_0^u f_e(v') 4\pi v'^2 dv' \,. \tag{1.186}$$

For readers who are not familiar with the discussion of the Poisson integral, we briefly present an "evaluation for pedestrians." Let us start with

$$\int \frac{\boldsymbol{u} - \boldsymbol{v}'}{|\boldsymbol{u} - \boldsymbol{v}'|^3} f_e(\boldsymbol{v}') d^3 v' = -\nabla_u \int \frac{1}{|\boldsymbol{u} - \boldsymbol{v}'|} f_e(\boldsymbol{v}') d^3 v' \,. \tag{1.187}$$

Next, we introduce spherical coordinates for the integration on the right-hand side, perform the integration over the azimuthal angle, obtaining after a simple reformulation

$$\begin{aligned}
&\int \frac{1}{|\boldsymbol{u} - \boldsymbol{v}'|} f_e(\boldsymbol{v}') d^3 v' \\
&= 2\pi \int_0^\infty dv' v'^2 \int_{-1}^{+1} d\left(\cos\vartheta'\right) \frac{d}{\cos\vartheta'} \sqrt{u^2 + v'^2 - 2uv'\cos\vartheta'} \left(-\frac{f_e(\boldsymbol{v}')}{uv'}\right) \\
&= 4\pi \left\{ \frac{1}{u} \int_0^u v'^2 f_e(\boldsymbol{v}') dv' + \int_u^\infty v' f_e(\boldsymbol{v}') dv' \right\} .
\end{aligned} \tag{1.188}$$

Applying the operator $-\nabla_u$ to the right-hand side, we obtain Eq. (1.186).

For small relative velocities compared to the thermal electron velocity, $u \ll v_{the}$, we obtain

$$\int_0^u f_e(v') 4\pi v'^2 dv' \approx f_e(0) \frac{4\pi}{3} u^3 \,, \tag{1.189}$$

and thereby for a Maxwellian

$$\boldsymbol{I} \approx \frac{\sqrt{2}}{3\sqrt{\pi}} \left(\frac{m_e}{T_e}\right)^{3/2} \boldsymbol{u} \,. \tag{1.190}$$

On the other hand, for large velocities u,

$$\boldsymbol{I} \sim \frac{\boldsymbol{u}}{u^3} \,. \tag{1.191}$$

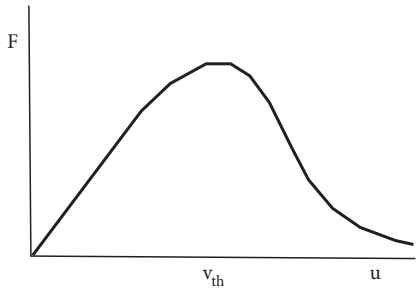

Figure 1.5 Sketch of the friction force as a function of the drift velocity u.

Summarizing for small velocities compared to the thermal electron velocity of the scatterers, the friction force is

$$\boldsymbol{F}_i = -\frac{1}{(4\pi\varepsilon_0)^2}\frac{4\sqrt{2\pi}}{3}\frac{Z^2\ln\Lambda e^4 n_e}{m_e}\left(\frac{m_e}{T_e}\right)^{3/2}\boldsymbol{u}\,, \tag{1.192}$$

that is, it increases in magnitude with velocity. However, when the drift velocity becomes larger than the thermal velocity, we get a decaying friction force, $F \sim u^{-2}$. Remember, u is the mean velocity difference. The friction force reaches some maximum around the electron thermal velocity; see Figure 1.5.

We now apply these results to the problem of current flow through plasma. At equilibrium, the driving force by the electric field must be equilibrated by the friction, that is, for ions

$$\boldsymbol{F}_i + Ze\boldsymbol{E} = 0\,. \tag{1.193}$$

However, when the drift velocity becomes much larger than the electron thermal velocity, collisions cannot stop particle acceleration, and the particles run away. In other words, when the applied electric field becomes large,

$$E > \frac{F_{max}}{Ze}\,, \tag{1.194}$$

we get runaway particles. The critical field is the Dreicer field

$$E_{Dr} \approx \frac{1}{(4\pi\varepsilon_0)^2}\frac{\ln\Lambda n_e e^3 Z}{T_e} \sim \ln\Lambda\frac{e}{\lambda_D^2}\,. \tag{1.195}$$

A more general kinetic evaluation gives [15]

$$E_{Dr} \approx \frac{0.43}{(4\pi\varepsilon_0)^2}\frac{2\pi\ln\Lambda n_e e^3 Z}{T_e} \approx 5.6\times10^{-18} n_e Z\frac{\ln\Lambda}{T_e}\left[\frac{V}{m}\right]\,. \tag{1.196}$$

In order to elucidate the typical behaviors for $u \ll v_{th}$ and $u \gg v_{th}$, respectively, we solve the momentum equation

$$m_i\frac{d\boldsymbol{u}}{dt} = \boldsymbol{F}_i + Ze\boldsymbol{E} \tag{1.197}$$

in the two regions. In both cases, we anticipate a one-dimensional description. In the small velocity range, the momentum equation is of the form

$$\frac{du}{dt} = -au + b \,, \tag{1.198}$$

(with constants a and b which are easy to determine). Its solution, for $u = u_0 = 0$ at $t = t_0 = 0$, is

$$u(t) = \frac{b}{a}\left(1 - e^{-at}\right) \to \frac{b}{a} \quad \text{for} \quad t \to \infty \,. \tag{1.199}$$

For small velocities (fields), one finds stationary conduction

$$j \sim enu \sim ne\frac{eE}{m\nu_{ei}} \sim \frac{\varepsilon_0\omega_p^2}{\nu_{ei}}E \sim \sigma E \,. \tag{1.200}$$

The conductivity is inversely proportional to the collision frequency. Since the latter decays with increasing temperature, we find

$$\sigma \sim T_e^{3/2} \,, \tag{1.201}$$

that is, the electric conductivity of hot plasmas becomes very large. The resistivity η is inversely proportional to σ, that is,

$$\eta = \frac{1}{\sigma} \,, \tag{1.202}$$

and thereby it decreases with temperature. The value obtained from kinetics [15] is

$$\eta \approx \frac{1}{(4\pi\varepsilon_0)^2}\frac{8\sqrt{\pi}\ln\Lambda Z e^2 m_e^{1/2}}{3\sqrt{2}T_e^{3/2}} \,. \tag{1.203}$$

For practical applications, we may use

$$\eta \approx 1.03 \times 10^{-4}\frac{Z\ln\Lambda}{T_e^{3/2}}\ \Omega\,\mathrm{m} \tag{1.204}$$

when T_e is measured in eV.

In the large velocity range, the momentum equation is of the form

$$\frac{du}{dt} = -\frac{g}{u^2} + b \tag{1.205}$$

(with constants g and b, which are easy to determine again). Its solution for $u = u_0 > \sqrt{g/b}$ at $t = t_0 = 0$ is

$$u - u_0 + \frac{1}{2}\sqrt{\frac{g}{b}}\ln\left[1 - 2\frac{\sqrt{\frac{g}{b}}}{u + \sqrt{\frac{g}{b}}}\right]_{u_0}^{u} = bt \,. \tag{1.206}$$

It is easy to see that t is a monotonously increasing function of u for $u > \sqrt{g/b}$. In other words,

$$u \to bt \quad \text{for} \quad t \to \infty \,. \tag{1.207}$$

This asymptotic reflects the so called runaway phenomenon.

1.5 Fusion Processes

Nuclear fusion is the source for energy production in burning stars. Fusion powers the sun and stars as hydrogen atoms fuse together to form helium, and matter is converted into energy. At low temperatures, fusion is not possible because the strongly repulsive electrostatic forces between the positively charged nuclei prevent them from getting close enough together for fusion to occur. However, if the conditions are such that the nuclei can overcome the electrostatic forces to the extent that they can come within a very close range of each other. Then, the attractive nuclear force between the nuclei will outweigh the repulsive (electrostatic) force, allowing the nuclei to fuse together.

In the sun, massive gravitational forces create the right conditions for fusion, but on earth they are much harder to achieve. Fusion fuel – different isotopes of hydrogen – must be heated to extreme temperatures of the order of 10^8 °C, and must be kept dense enough and confined for long enough in order to allow the nuclei to fuse. The aim of the controlled fusion research program is to achieve "ignition," which occurs when enough fusion reactions take place for the process to become self-sustaining, with fresh fuel then being added to continue it.

The binding energy per nucleon is the key to the understanding of fusion as an energy source. Light nuclei may fuse to heavier nuclei, releasing energy in the form of kinetic energy and radiation. When plotting the binding energy per nucleon, as depicted in Figure 1.6, we recognize that the curve has a minimum. On the left-hand side of Figure 1.6, the sum of the masses of two fusion components is larger than the mass of the fusion product. The mass defect Δm corresponds to an energy difference $\Delta E \equiv B = \Delta m c^2$. The binding energy per nucleon B/A, where A is the nucleon number (rough atomic weight), has a minimum near $A \approx 56$. The elements close to this atomic number are exceedingly stable.

With current technology, the reaction most readily feasible is between the nuclei of the two heavy forms (isotopes) of hydrogen-deuterium (D) and tritium (T). The deuterium-tritium reaction possesses a favorable cross section. Each D-T fusion event releases approximately 17.6 MeV ($2.8 \times 10{-}12$ J, compared with 200 MeV for a U-235 fission), that is,

$$\mathrm{D} + \mathrm{T} \to {}^4\mathrm{He}\ (3.5\ \mathrm{MeV}) + \mathrm{n}\ (14\ \mathrm{MeV}) \tag{1.208}$$

Deuterium occurs naturally in seawater ($30\,\mathrm{g/m^3}$), which makes it very abundant relative to other energy resources. Tritium does not occur naturally and is radioactive, with a halflife of around 12 yr. It can be made in a conventional nuclear reactor,

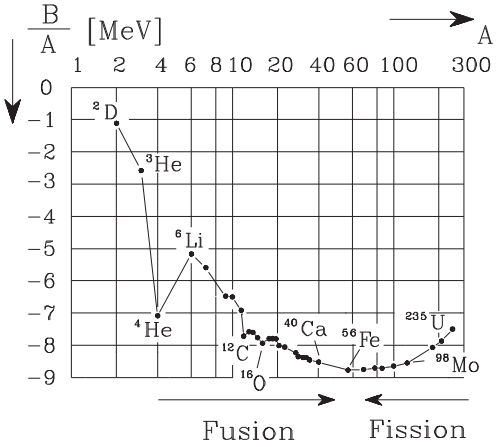

Figure 1.6 Binding energy per nucleon as a function of the number of nucleons *A*.

or in the present context, bred in a fusion system from lithium,

$$^6\mathrm{Li} + n \rightarrow {}^4\mathrm{He} + \mathrm{T} \tag{1.209}$$

Lithium is found in large quantities (30 ppm) in the Earth's crust and in weaker concentrations in the sea.

Present estimates show that a *G W*-reactor needs approximately 100 kg D and 400 kg Li per year. In other words, the perspectives of controlled thermonuclear fusion become plausible when estimating that a few liters of seawater and some pieces of rock (order of kg for the lithium extraction) will be sufficient for the energy consumption of a family of four persons during one year. At present, two main experimental approaches are being studied: magnetic confinement and inertial confinement. The first method uses strong magnetic fields to contain the hot plasma. The second involves compressing a small pellet containing fusion fuel to extremely high densities using strong lasers or particle beams.

Although fusion does not generate long-lived radioactive products (and the unburned gases can be treated on site), there appears a short-term radioactive waste problem due to activation of the structural materials. Some component materials will become radioactive during the lifetime of a reactor due to bombardment with high-energy neutrons, and will eventually become radioactive waste. The volume of such waste would be similar to the corresponding volumes from fission reactors. However, the longterm radiotoxicity of the fusion wastes would be considerably lower than that from actinides in used fission fuel. The fast neutron problem triggered other scenarios which are also discussed from time to time in the public [35]. One is the recovery of ^{3}He (consisting of two protons and one neutron) from the surface of the moon. ^{3}He is practically not available on the earth; tritium decays into ^{3}He with a 12 yr halflife. However, cosmic rays, originating from the solar wind, already penetrating for billions of years approximately 1 m into the surface of the moon produced ^{3}He there due to the spallation process. The fusion of D with ^{3}He

to ^{4}He is a possible process, without producing significant neutrons. The cross section for the D–^{3}He reaction is, however, smaller by a factor 10 than the cross section for D–T fusion.

1.5.1 Fusion Processes in Burning Stars

Stellar fusion processes were already discussed a long time ago. Among the first authors are Atkinson and Houtermans [36]. Laboratory observations go back to the 1930s. At the end of the 1930s, Weizsäcker and Bethe found the dominating processes responsible for the burning in stars [18].

We have to differentiate between massive and low-mass stars; the borderline is approximately at the order of the mass of our sun. In low-mass stars, the fusion cycle starts with the proton–proton reaction

$$\mathrm{p} + \mathrm{p} \rightarrow \mathrm{D} + \mathrm{e}^+ + \nu \tag{1.210}$$

After that, the deuteron may again react with a proton

$$\mathrm{D} + \mathrm{p} \rightarrow {}^3\mathrm{He} + \gamma \ , \tag{1.211}$$

leading to the already mentioned ^{3}He fusion

$${}^3\mathrm{He} + {}^3\mathrm{He} \rightarrow {}^4\mathrm{He} + 2\mathrm{p} \tag{1.212}$$

For massive stars, that process does not deliver enough energy to sustain the necessary pressure. The compression of massive stars continues, transforming gravitational energy into kinetic energy. Using in the virial theorem $-3\langle P\rangle V \approx E_{gr} < 0$ and $\langle P\rangle V \approx N k_B T$, we obtain for the kinetic energy $E_{kin} \approx 3/2 N k_B T$

$$E_{kin} \approx -\frac{1}{2} E_{gr} > 0 \ . \tag{1.213}$$

The latter relation makes, for massive stars, the increase in temperature plausible.

At higher temperatures, a new process becomes possible, the CNO cycle (for carbon-nitrogen-oxygen), or sometimes Bethe–Weizsäcker cycle, with a much higher fusion power than the direct proton–proton reaction just mentioned. The CNO process was proposed by Carl von Weizsäcker and Hans Bethe independently in 1938 and 1939, respectively [18]. Models show that the CNO cycle is the dominant source of energy in stars heavier than about 1.5 times the mass of the sun. The previously mentioned proton–proton chain is more important in stars of the mass of the sun or less. This distinction stems from differences in temperature dependency between the two reactions; the p–p reactions start occurring at lower temperatures, making it dominant in smaller stars. The CNO chain starts occurring at higher temperatures, but its energy output rises much faster with increasing temperatures. That crossover is depicted in Figure 1.7.

In the CNO cycle, four protons fuse, using carbon, nitrogen and oxygen isotopes as a catalyst, to produce one alpha particle, two positrons and two electron

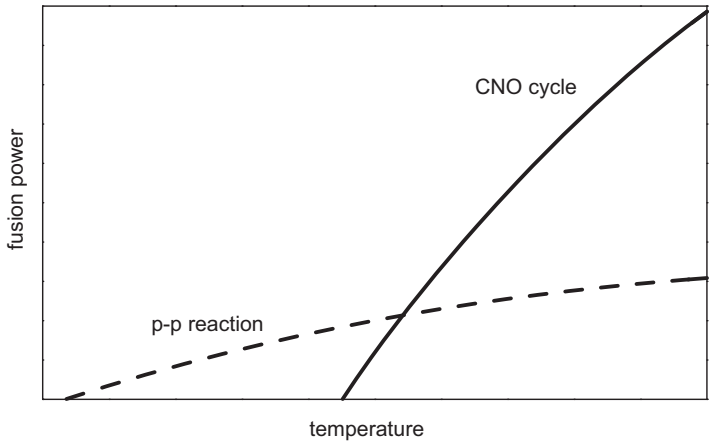

Figure 1.7 Temperature dependence of the fusion power in the p–p reaction and the CNO cycle, respectively.

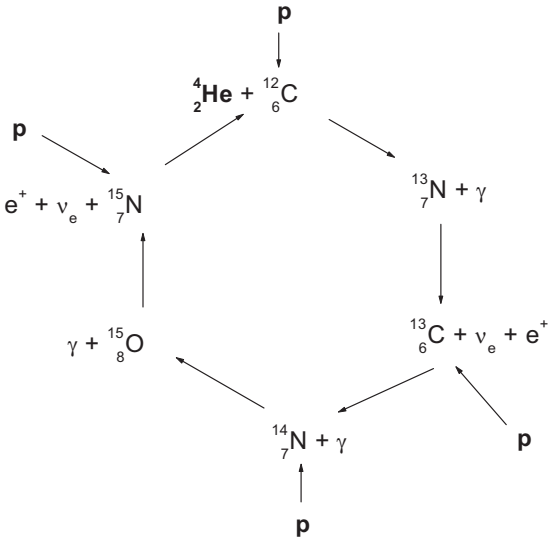

Figure 1.8 Diagram of the CNO cycle. The reaction chain starts at top and should be read clockwise.

neutrinos. The positrons will almost instantly annihilate with electrons, releasing energy in the form of gamma rays. The neutrinos escape from the star carrying away some energy. The carbon, nitrogen, and oxygen isotopes are in effect one nucleus that goes through a number of transformations in an endless loop, as shown in Figure 1.8.

Our sun (mass density 160 g cm^{-3}) is confined by gravitation, the primary heating was due to compression. The core temperature is around 15.7×10^6 K and

only 1.7% of ^{4}He nuclei produced in the sun are born in the CNO cycle. The p–p chain reaction is by far dominating. The fusion power density is approximately $0.28\,\mathrm{mW\,cm^{-3}}$.

During the p–p reaction,

$$\mathrm{p} + \mathrm{p} \rightarrow \mathrm{D} + \mathrm{e}^+ + \nu_e \tag{1.214}$$

$$\mathrm{p} + \mathrm{D} \rightarrow {}^3\mathrm{He} + \gamma \tag{1.215}$$

$${}^3\mathrm{He} + {}^3\mathrm{He} \rightarrow {}^4\mathrm{He} + \mathrm{p} + \mathrm{p} \tag{1.216}$$

the energy gain per produced ^{4}He nucleus is $26\,\mathrm{MeV} \mathrel{\hat{=}} 26 \times 1.6 \times 10^{-13}\,\mathrm{J}$. The radiation power of the sun is $4 \times 10^{26}\,\mathrm{W}$.

It is interesting to note that the p–p reaction is rather slow. A proton needs approximately $5 \times 10^9\,\mathrm{yr} = 1.5 \times 10^{17}\,\mathrm{s}$ to fuse with another proton. One needs four protons to effectively create a ^{4}He nucleus with 26 MeV energy gain. For the total power of $4 \times 10^{26}\,\mathrm{W}$, one needs

$$\frac{4 \times 4 \times 10^{26}}{26 \times 1.6 \times 10^{-13}} = 4 \times 10^{38}\,\frac{\text{protons}}{\mathrm{s}}\,. \tag{1.217}$$

2×10^{38} neutrinos per second are produced. Part of them will reach the Earth. (The neutrino problem is a separate issue.)

Dividing the power $4 \times 10^{26}\,\mathrm{W}$ by the mass of the sun, we get the average 0.2 mW/kg. That power density is smaller than the corresponding one of a human body. We may estimate the total number of protons in the sun as 7×10^{56}. One needs $4 \times 10^{38}\,\mathrm{s^{-1}}$ for the total power $10^{38} \times 26 \times 1.6 \times 10^{-13} = 4 \times 10^{26}\,\mathrm{W}$. $7 \times 10^{56}/4 \times 10^{38} \approx 2 \times 10^{18}\,\mathrm{s} \approx 63\,\mathrm{Gyr}$ is the upper limit for the lifetime of the sun. Actually, the lifetime may be smaller by a factor of ten since not all protons will fuse.

The sun is essentially a quite stable burning object. It can be considered as a self-regulating thermostat. In case the energy release and thereby the temperature in the interior increases, the total energy $E = E_{kin} + E_{gr}$ increases. Because of Eq. (1.213), we have

$$E \approx \frac{1}{2} E_{gr} \approx -E_{kin}\,. \tag{1.218}$$

Thus, with increasing energy, also the gravitational energy increases and the kinetic energy (temperature) decreases. The sun expands and cools, acting in the opposite direction to the initial disturbance. On the other hand, when the energy production in the interior becomes smaller, the total energy decreases. The sun would contract and increase its temperature; again, a reaction which opposes the original disturbance.

When the fuel for p–p fusion, often called hydrogen burning, is running low in the core, the sun will contract and becomes hotter. Then, the hydrogen burning can also take place in the previously colder outer shells. The next dominating process

Table 1.1 Possible fusion products are shown in dependence of temperature T and mass M of a star.

$T = 10^7$ K $M > 0.08 M_\odot$	hydrogen	→	helium
$T = 10^8$ K $M > 1/2 M_\odot$	helium	→	carbon, oxygen
$T = 5 \times 10^8$ K $M > 8 M_\odot$	carbon	→	oxygen, neon, ...
$T = 10^9$ K	neon	→	oxygen, magnesium
$T = 2 \times 10^9$ K	oxygen	→	magnesium, ... sulfur
$T = 3 \times 10^9$ K $M > 11 M_\odot$	silicon	→	iron, ...

in the core will be helium burning. Temperatures of approximately 2×10^8 K will become possible in the center; the maximum mass density will be of the order $10^8\,\mathrm{kg\,m^{-3}}$. The sun will appear as a red giant. That terminology becomes plausible because of the following typical values for luminosity, surface temperature, and radius, namely, roughly $L = 1000\,L_\odot$, $T_O = 4000$ K, $R = 70\,R_\odot$, respectively.

Stars with masses above $0.5\,M_\odot$ will follow this scenario. Depending on the mass of the star, further steps are possible as depicted in Table 1.1.

As discussed, the highest element in this fusion scenario will be ^{56}Fe. Heavier elements can be generated by neutron capture and subsequent β-decay of the neutron into a proton and an electron.

During the cosmological evolution, the situation occurred in which temperatures were high enough, but the mass densities were too low to enable fusion. Only after the formation of massive stars can fusion become possible.

When all the fuel for fusion runs dry, the stars will further shrink. For stars with intermediate masses like the sun, degenerate electrons may provide the pressure for hindering a complete collapse. The quantum description becomes necessary. Whether it should be nonrelativistic or relativistic is an important question; the answer depends on the mass of the star. In the ultrarelativistic regime, for example, the equilibrium with a pressure delivered by degenerate electrons is fragile. For masses smaller than $1.4\,M_\odot$ (Chandrasekhar mass), a nonrelativistic description is appropriate, and the final state of our sun will be a compact object with degenerate electrons providing the pressure for equilibrium. Such an object is called a white dwarf; typical parameters are $L = L_\odot/100$, $T_O = 16\,000$ K, $R = R_\odot/70$, $\rho \approx 10^9\,\mathrm{kg\,m^{-3}}$.

For massive stars, the pressure of degenerate electrons will not be sufficient. The star shrinks further, ending, for example, as a neutron star. Degenerate neutrons in the nonrelativistic regime become responsible for the necessary pressure. Mass densities of order 10^{14}–$10^{17}\,\mathrm{kg\,m^{-3}}$ are typical, temperatures may reach 10^8 K. A typical radius is 17 km.

Similar to the applicability of the model of a white star, not all massive stars will end as a neutron star. An upper limit of the order $M \approx 3\,M_\odot$ exists. If the masses are larger, the neutrons become ultrarelativistic and the equilibrium is fragile. Such supermassive stars may end as black holes.

When comparing with other energy energy providers, we cite $0.2\,\mathrm{W/cm^3}$ for a coal-fired power plant and $90\,\mathrm{W/cm^3}$ for a light-water reactor. For our sun, the estimate for the center is $3.5 \times 10^{-6}\,\mathrm{W/cm^3}$ (averaged over the whole sun volume we would get $2.7 \times 10^{-7}\,\mathrm{W/cm^3}$).

For details on the fusion window, fusion power rates, cross sections, and so on, we refer to more detailed reports, for example, [14, 18, 19, 37].

1.5.1.1 Ignition Conditions for a Fusion Plasma

We conclude this section by a short summary of the Lawson criterion [32]. The total thermal energy of a plasma consisting of electrons and ions in equal numbers is

$$W = \int dV 3nT \equiv 3\overline{nT}V \,. \tag{1.219}$$

The energy loss rate P_L defines the energy confinement time τ_E via

$$P_L = \frac{W}{\tau_E} \,. \tag{1.220}$$

When in a stationary state the energy loss is balanced by additional heating,

$$P_H = P_L \,, \tag{1.221}$$

we obviously have

$$\tau_E = \frac{W}{P_H} \,. \tag{1.222}$$

However, besides additional (external) heating, we should also take into account alpha particle heating. A fraction of the fusion energy is taken over by the $^4\mathrm{He}(\alpha)$ particles. The α particles are charged, in contrast to the neutrons. The charged particles interact with the plasma, transferring part of the 3.5 MeV ($= E_\alpha$) to electrons and ions. The α particle heating is defined via the heating power

$$P_\alpha = \frac{1}{4}\overline{n^2 \langle \sigma \mathrm{v} \rangle} V E_\alpha \,, \tag{1.223}$$

where $\langle \sigma \mathrm{v} \rangle$ is the reaction parameter [37]. In a stationary state with α particle heating plus additional heating, the power balance would be

$$P_H + P_\alpha = P_L \tag{1.224}$$

or

$$P_H = \left(\frac{3nT}{\tau_E} - \frac{1}{4} n^2 \langle \sigma \mathrm{v} \rangle E_\alpha \right) V \,, \tag{1.225}$$

where, on the right-hand side, for the reason of simplicity, the indication of volume averaging has been omitted. Self-contained burning (or ignition with $P_H = 0$) occurs for

$$n\tau_E \geq \frac{12}{\langle \sigma \mathrm{v} \rangle} \frac{T}{E_\alpha} \sim T e^{\mathrm{const}/T^{1/3}} \,. \tag{1.226}$$

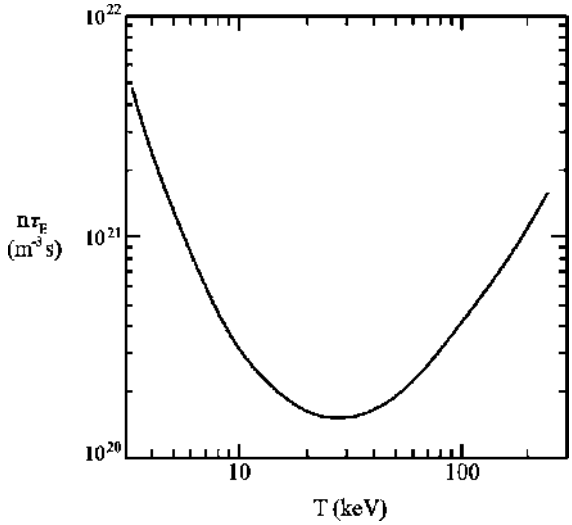

Figure 1.9 $12T/(\langle\sigma v\rangle E_\alpha)$ as a function of T.

The right-hand side is a function of temperature, as shown in Figure 1.9. The minimum of $12T/(\langle\sigma v\rangle E_\alpha)$ occurs at $T \approx 30\,\mathrm{keV}$; taking this value, we find

$$n\tau_E \geq 1.5 \times 10^{20}\,\mathrm{m}^{-3}\,\mathrm{s}\,. \tag{1.227}$$

This relation is known as the Lawson criterion.

Still, τ_E depends on temperature and other variables. In other words, on the transport properties in the plasma. One can take advantage of the fact that in the temperature region

$$10\,\mathrm{keV} \leq T \leq 20\,\mathrm{keV}\,, \tag{1.228}$$

one may approximate

$$\langle\sigma v\rangle \approx 1.1 \times 10^{-24}\,T^2\,\mathrm{m}^3\,\mathrm{s}^{-1} \tag{1.229}$$

when measuring T in keV. Within this approximation, the ignition criterion can be written in the form

$$nT\tau_E \geq 3 \times 10^{21}\,\mathrm{m}^{-3}\,\mathrm{keV\,s}\,. \tag{1.230}$$

For example, at $n = 10^{20}\,\mathrm{m}^{-3}$, $T = 10\,\mathrm{keV}$, the energy confinement time should be larger than 3 s.

To measure the progress in nuclear fusion research, the Q-factor

$$Q = \frac{5P_\alpha}{P_H} \tag{1.231}$$

has been introduced. Note that the factor $5 = 17.5/3.5 \approx E_{fus}/E_\alpha$ takes care of the whole energy gain and not only the part carried by the α-particles. $Q \to \infty$ means ignition.